Title
Probing Charge Transport through Peptide Bonds

Journal
The Journal of Physical Chemistry Letters, 9(4)

ISSN
1948-7185

Authors
Brisendine, Joseph M
Refaely-Abramson, Sivan
Liu, Zhen-Fei
et al.

Publication Date
2018-02-15

DOI
10.1021/acs.jpclett.8b00176

Peer reviewed

Published in final edited form as:

J Phys Chem Lett. 2018 February 15; 9(4): 763–767. doi:10.1021/acs.jpclett.8b00176.

Probing Charge Transport through Peptide Bonds

Joseph M. Brisendine[†,‡], **Sivan Refaely-Abramson**[†,¶], **Zhen-Fei Liu**[†,¶], **Jing Cui**[§], **Fay Ng**[‖], **Jeffrey B. Neaton**[¶,⊥], **Ronald L. Koder**[‡,#], and **Latha Venkataraman**[‖,@]

[‡]Graduate Programs of Physics, Biology, Chemistry and Biochemistry, The Graduate Center of CUNY, New York, and Department of Biochemistry, City College of New York, New York.

[¶]Molecular Foundry, Lawrence Berkeley National Laboratory; Department of Physics, University of California Berkeley, Berkeley, CA 94720, USA

[§]Department of Physics, Columbia University, New York, NY

[‖]Department of Chemistry, Columbia University, New York, NY

⊥ Kavli Energy Nanosciences Institute at Berkeley, Berkeley, CA 94720, USA

[#]Department of Physics, City College of New York, New York, NY

[@]Department of Applied Physics, Columbia University, New York, NY

Abstract

We measure the conductance of unmodified peptides at the single molecule level using the scanning tunneling microscope-based break-junction method, utilizing the N-terminal amine group and the C-terminal carboxyl group as gold metal-binding linkers. Our conductance measurements of oligoglycine and oligoalanine backbones do not rely on peptide side-chain linkers. We compare our results with alkanes terminated asymmetrically with an amine group on one end and a carboxyl group on the other to show that peptide bonds decrease the conductance of an otherwise saturated carbon chain. Using a newly-developed first-principles approach, we attribute the decrease in conductance to charge localization at the peptide bond, which reduces the energy of the frontier orbitals relative to the Fermi energy and the electronic coupling to the leads, lowering the tunneling probability. Crucially, this manifests as an increase in conductance decay of peptide backbones with increasing length when compared with alkanes.

Graphical Abstract

[†]These authors contributed equally

Supporting Information

Additional conductance-displacement histograms, further explanation of the extended DFT+Σ computational method, and full computational details.

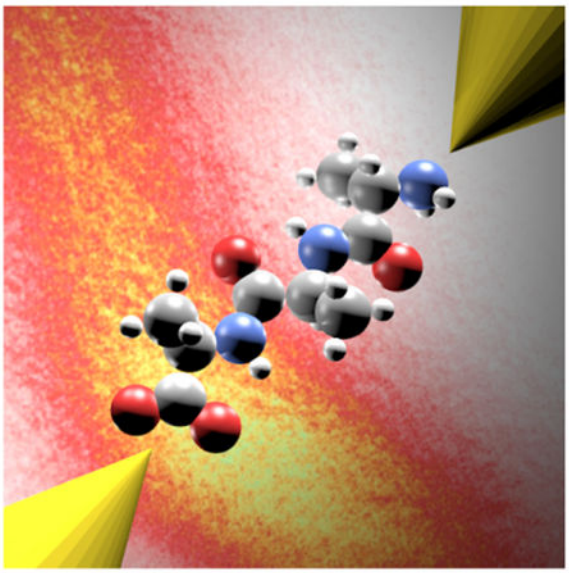

Biological molecules play central roles in the complex and elegant charge transport processes that underlie cellular respiration, photosynthesis, and energy storage. Such processes are often facilitated through inter- or intra-protein and peptide electron transfer.[1–8] When tunneling (super-exchange) is the predominant transfer mechanism, transfer rates decay exponentially with distance with a characteristic decay constant which should depend on the intervening peptide structure and composition.[9–12] However, the specific nature and magnitude of electron transfer along the peptide backbone remains uncertain and is not well studied. Previous experiments attempting to probe the intrinsic backbone conductance measured transport through high-concentration peptide monolayers on Au, where both intramolecular interactions and binding groups may obscure native peptide conductance.[5,6,13,14] Prior single-molecule conductance measurements of individual peptides[4,5] were carried out with non-native linkers such as alkyl thiols[14,15] or in non-native arrangements such as two thiol-containing amino acids (cysteines)[16–18] to facilitate stronger peptide-electrode binding, leaving open questions as to whether they are observing native transport behavior of the peptide backbone. Prior conductance measurements of short amino acids[19,20] without artificial linkers did not report the length dependence of the conductance decay or compare these to saturated carbon backbones.

Here, we demonstrate single molecule conductance measurements of unmodified peptides in their native solvent, water, and establish their intrinsic conductance at the single molecule level. We use the scanning tunneling microscope based break-junction method[16,21,22] to measure the conductance of oligoglycine and oligoalanine, and compare them with measurements on alkanes. We utilize the amine group at the N-terminus[23] and the carboxyl group at the C-terminus as gold-binding linkers allowing us to directly measure the conductance of native peptides bound to gold electrodes at the single-molecule level.[19,24–26] We show that the peptide backbone is less conductive than an alkane chain of equal length.[14,27,28] Using first principles calculations, we show that the decrease in conductance can be attributed to charge localization at the peptide bond which is also modified by the amino

acid side chain. Crucially, this manifests as an increase in conductance decay of peptide backbones with increasing length.

We carried out scanning tunneling microscope based break-junction (STM-BJ) measurements as illustrated in Figure 1a on a series of peptides and alkanes.[21,22] In these measurements, an Au STM tip was repeatedly driven in and out of contact of an Au substrate while the current across the tip/sample junction was recorded at a fixed bias to generate a conductance (current/voltage) versus displacement trace. Histograms of these traces were constructed from thousands of traces to assess the most frequently observed conductance as well as its dependence on junction elongation length. The target peptide or alkane was introduced on the STM substrate from dilute (1mM) solutions in water (pH 7) or CHES buffer (pH 9). The peptides and aminocarboxy-alkanes were purchased from Sigma-Aldrich, assayed for purity using C18 high performance liquid chromatography (HPLC), and then either purified by HPLC or used as purchased (if the purity was 98% or greater). Since the measurements were carried out in an ionic environment, the gold STM tip was first coated with an insulating wax (Apiezon) to prevent Faradaic currents from masking the molecular junction currents.[29]

We show, in Figure 1b, sample conductance traces measured with tri-alanine (**AAA**) where plateaus are visible between 10^{-5} and 10^{-6} G_0 ($G_0 = 2e^2/h$ is the quantum of conductance). These measurements were carried out in pH 7 water and indicate that we can trap an **AAA** between two gold electrodes through the formation of a donor-acceptor bond between the amine group and gold on one end, and between a carboxyl group and gold on the other end. These junctions can be formed only when the amine group is neutral (NH_2) and the carboxyl group is negatively charged (COO^-), and this is achieved when the solution pH is 7 or higher.[26] We stress here that we are probing the conductance of the peptide backbone, and not the side chain, by directly forming a bond between the electrode and the N- or C-terminus of the peptide. This is in contrast to prior work where the thiol group of a cystein side chain was used to contact the metal electrode.[4,16]

Figure 1c analyzes 6000 **AAA** junction conductance traces without any data selection in the form of a two-dimensional conductance-displacement histogram created by aligning traces at the location where the gold point-contact ruptures. We see that **AAA** junctions can sustain an elongation of about 5 Å, which is indicative of a junction formed with a molecular backbone that is ~10Å in length.[30]

To understand the impact of the peptide bonds on charge transfer, we first compare the result of **AAA** (tri-alanine) with conductance measurements of two other molecules, **C7** (Amino-octanoic acid) and **F1** (5-(alanylamino)pentanoic acid), both terminated with an NH_2 and a COOH group and both with the same number of atoms (C or N) in the backbone. **C7** is a seven-carbon alkyl chain while **F1** contains a single alanine bound through a peptide bond to an alkyl chain with 4 carbons as shown in Figure 2a and was synthesized according to literature.[31] We compare, in Figure 2b, conductance histograms obtained from STM-BJ measurements with these three molecules. These data show unambiguously that the conductance of **C7** is the largest while that of **AAA** is the smallest with **F1** being intermediate. Since the histogram for **C7** shows two clearly distinguishable peaks, we fit this

histogram with a sum of Gaussian (or normal) distributions. We find that using three such Gaussians gives us the best fit (see SI Figure S1a). The peaks of the three Gaussian distributions are at $2.3\times 10^{-5}G_0$, $4.6\times 10^{-5}G_0$ and $8\times 10^{-5}G_0$, indicating that we are likely forming one-, two- or three-molecule junctions. The data for **F1** can be fit with two Gaussians (see SI Figure S1b) where we again see that the 2 peak conductance values are about a factor of 2 different, indicating that we can trap either one or two molecules in parallel.[32] However, for **AAA**, we cannot distinguish multi-molecule junctions in the histogram. Measurements at lower concentration did not yield clear conductance peaks in the histogram and therefore we conclude that we are likely measuring one or two molecular junctions. We fit a single peak to the histogram to determine its conductance and this serves as an upper bound. We find that the single-molecule junction conductance is highest for **C7** and lowest for **AAA**. This result is contrary to a simplistic assumption that adding a peptide bond to a saturated chain will add conjugated character thereby increasing conductance (see discussion in Ref.[6]).

To understand the impact of peptide bonds on their ability to conduct, we characterize the conductance decay as a function of length for oligoalanine and oligoglycine and compare these with measurements of alkanes. Figure 3a and 3b depicts 1D conductance histograms from measurements of alanine and glycine respectively, with 1 (**A**, **G**), 2 (**AA**, **GG**), and 3 (**AAA**, **GGG**) amino acids (2D histograms are provided in the supporting information document, Figure S2). We compare these data with measurements of alkane chains (**C1** - **C7**) in Figure 3c. The conductance for all three systems decreases with increasing molecular length. The conductance histograms for glycine and the alkanes show evidence for the formation of junctions with one, two and sometimes three molecules as discussed above and indicated by arrows for **GG** and **C5**, with the conductance of the two-molecule junction almost exactly twice that of the one-molecule junction. We fit these data with either a single (for alanine) or a multiple-Gaussian (for glycine and alkanes) and obtain the single-molecule conductance value for each system. These are plotted against calculated molecular length in the corresponding insets on a semi-logarithmic scale. Since we expect an exponential decay of conductance with length as $G \sim e^{-\beta L}$, we fit these data with a line and extract the β parameter for each series. We find that the beta for alkanes is the smallest at 0.75 ± 0.02/Å and comparable to measurements of alkanes with symmetric linker groups.[21,33] Glycine has β =0.97 ± 0.01/Å and alanine has β =0.93 ± 0.04/Å, both clearly larger than that of the alkane. Importantly, these results demonstrate that peptide side-chain identity and backbone conductance are not independent.

We now turn to first-principles calculations of coherent tunneling transport to elucidate the origin of the conductance trends found above. We compute the linear-response transmission and conductance of the molecular junctions considered here using a new *ab initio* approach based on density functional theory (DFT), the non-equilibrium Green's function (NEGF)[34] formalism, and a generalized version of DFT+Σ,[23] a GW-based self-energy correction[35] that can account quantitatively for exchange and correlation effects missing from DFT Kohn-Sham eigenstates, leading to predicted transmission functions and conductance values in far better agreement with experiments. As DFT+Σ requires as input electron addition and removal energies of a gas-phase reference molecule, and since the Au-COO^- bond is

covalent in nature, there is ambiguity in the gas-phase reference; here, we use the peptide plus three gold atoms at the COO^- linker as a super molecular reference, to properly account for the covalent molecule-lead binding. (Further details of our computational approach are provided in the supporting information.) Atomistic junction structures are constructed with the molecules forming chemical bonds to undercoordinated Au atoms. A typical junction structure and binding motifs are shown in the SI (Figure S3 and S4). Junction geometries are relaxed using DFT within the Perdew-Burke-Ernzerhof (PBE)[36] functional as implemented in SIESTA.[37] An optimal binding motif is found for a model system and used for all systems. Pseudopotentials and basis sets are adapted from previous work.[23] Periodic boundary conditions with 4×4×1 k-point sampling are used in all relaxations. Transport calculations are carried out using TranSIESTA,[34] with seven layers of gold on each side of the junction in the periodic unit-cell. DFT energy levels are corrected using a new OT-RSH based DFT+Σ approach,[38] generalized here for the case of covalent binding (see SI for details).

In Figure 4, we show zero-bias transmission functions, computed with DFT+Σ as described above, for **AAA**, **GGG**, and **C7** (see SI Figure S5 for the transmission curves of other junctions). The peak at around 2 eV below the Fermi energy, E_F, dominates the transmission at E_F and indicates that holes are the majority carriers for off-resonant coherent tunneling in these systems. The eigenchannels associated with these peaks are of similar nature for all junctions, and has a considerable contribution from charge distributed on the covalent binding of Au-COO^-. Using the calculated DFT+Σ transmission at E_F, we determine decay parameters for the series studied. These are shown in the inset of Figures 4a–4c. We find that the alkanes have the smallest decay constant of 0.69/A, while the two peptides both have larger computed decay parameters of 0.93/A, in good agreement with the measured experimental values of 0.75/Å for alkanes, and 0.93/A, 0.97/Å for alanine and glycine junctions, respectively. The comparative trend is directly related to enhanced presence and role of electronic states at the peptide bond for longer peptide molecules.

The calculated and measured conductance values are close in magnitude (see SI Table S1), and give a similar trend: while for short peptides (**C1/G** and **A**), the conductance is almost identical, the longer peptides show a discernable difference. This difference originates with the peptide bonds in the longer systems (**AA, AAA, GG,** and **GGG**), which are absent in the alkane series. For the longer peptides, the electronic states on the molecule dominating the transmission peaks are no longer localized primarily at the junctions covalent Au-O bond. Instead, there are significant contributions to that peak from charge localized at the peptide bonds, specifically O and N atoms (Figure 4b and 4c). As shown in Figure 4 (top), the charge distribution of the peptides is not of delocalized **π**-character, but rather localized on high-affinity atoms participating in the peptide bond. The difference in localization was also used in Ref.[39] to explain the conductance trends of alkane compared to oligoether molecules. It was recently shown that peptide bonds induce a large molecular dipole, causing charge localization,[14,40] which has long been understood to be a major driving force in secondary structure formation.[41] The decrease in conductance is associated with tightly-bound electronic states at the peptide bond. This reduces the energy of these states relative to

E_F and weakens the covalent bonds to the leads, lowering the peak transmission energy and reducing the electronic coupling, leading to a smaller tunneling probability.

An immediate significance of this work is proof-of-principle that unmodified biological molecules in a native environment can be analyzed with the STM break-junction method. Our biologically relevant measurements of peptide backbone conductance should be of use in improving reference values for transport calculations through larger proteins, complementary to measurements on molecular monolayers. Given the applicability of the STM method for native peptides, the variance in conductance of the natural amino acids becomes an immediately accessible subject for experimental investigation, and provides clarity to existing debates in the literature.

Our results already demonstrate that using the N and C termini as contacts unmasks side chain-dependent backbone conductance effects that are hidden by the use of sulfur-gold contacts, proving that side-chain identity and backbone conductance are not completely independent. This work thus opens new avenues of experimental investigation into the electron transport properties of protein structure.

Supplementary Material

Refer to Web version on PubMed Central for supplementary material.

Acknowledgments

The experimental work was supported in part by the National Science Foundation (award no. DMR-1507440). SRA acknowledges Rothschild and Fulbright fellowships. RLK acknowledges support via National Institutes of Health grant 1R01-GM111932 and the program and infrastructure support from the National Institutes of Health National Center for Research Resources to the City College of New York (5G12MD007603–30). RLK is a member of the New York Structural Biology Center (NYSBC). The computational part of this work was supported by the U.S. Department of Energy, Office of Basic Energy Sciences, Materials Sciences and Engineering Division, under Contract No. DE-AC02–05CH11231. A portion of this work was also supported by the Molecular Foundry through the U.S. Department of Energy, Office of Basic Energy Sciences, under the same contract number. A portion of the computation work was done using NERSC resources.

References

(1). Gray HB; Winkler JR Electron tunneling through proteins. Q. Rev. Biophys 2003, 36, 341–372. [PubMed: 15029828]

(2). Cordes M; Giese B Electron transfer in peptides and proteins. Chem. Soc. Rev 2009, 38, 892–901. [PubMed: 19421569]

(3). Falkowski PG; Fenchel T; Delong EF The microbial engines that drive Earth's biogeo-chemical cycles. Science 2008, 320, 1034–1039. [PubMed: 18497287]

(4). Sek S Review peptides and proteins wired into the electrical circuits: An SPMbased approach. Biopolymers 2013,100, 71. [PubMed: 23335169]

(5). Juhaniewicz J; Pawlowski J; Sek S Electron transport mediated by peptides immobilized on surfaces. Isr. J. Chem 2015, 55, 645.

(6). Amdursky N; Marchak D; Sepunaru L; Pecht I; Sheves M; Cahen D Electronic Transport via Proteins. Adv. Mater 2014, 26, 7142. [PubMed: 25256438]

(7). Amdursky N Electron Transfer across Helical Peptides. Chem. Plus Chem. 2015, 80, 1075.

(8). Scullion L; Doneux T; Bouffier L; Fernig DG; Higgins SJ; Bethell D; Nichols RJ Large conductance changes in peptide single molecule junctions controlled by pH. J. Phys. Chem. C 2011,115, 8361–8368.

(9). Onuchic JN; Beratan DN; Winkler JR; Gray HB Pathway Analysis of Protein Electron-Transfer Reactions. Ann. Rev. Biophys 1992, 21, 349–377.

(10). Prytkova TR; Kurnikov IV; Beratan DN Coupling coherence distinguishes structure sensitivity in protein electron transfer. Science 2007, 315, 622–625. [PubMed: 17272715]

(11). Schlag EW; Sheu SY; Yang DY; Selzle HL; Lin SH Distal charge transport in peptides. Angew. Chem. Int. Ed 2007, 46, 3196–210.

(12). Malak RA; Gao Z; Wishart JF; Isied SS Long-range electron transfer across Peptide bridges: the transition from electron superexchange to hopping. J. Am. Chem. Soc 2004,126, 13888–9. [PubMed: 15506726]

(13). Thuo MM; Reus WF; Simeone FC; Kim C; Schulz MD; Yoon HJ; White-sides GM Replacing CH2CH2 with CONH Does Not Significantly Change Rates of Charge Transport through AgTS-SAM//Ga2O3/EGaIn Junctions. J. Am. Chem. Soc 2012, 134, 10876–10884. [PubMed: 22676159]

(14). Sepunaru L; Refaely-Abramson S; Lovrincic R; Gavrilov Y; Agrawal P; Levy Y; Kronik L; Pecht I; Sheves M; Cahen D Electronic Transport via Homopeptides: The Role of Side Chains and Secondary Structure. J. Am. Chem. Soc 2015,137, 9617–26. [PubMed: 26149234]

(15). Uji H; Morita T; Kimura S Molecular direction dependence of single-molecule conductance of a helical peptide in molecular junction. Phys. Chem. Chem. Phys 2013,15, 757. [PubMed: 23202534]

(16). Xiao X; Xu B; Tao N, Conductance Titration of Single-Peptide Molecules. J. Am. Chem. Soc 2004, 126,5370–5371. [PubMed: 15113203]

(17). Juhaniewicz J; Sek S Peptide molecular junctions: Electron transmission through individual amino acid residues. J. Electroanal. Chem 2010, 649, 83–88.

(18). Juhaniewicz J; Sek S Peptide molecular junctions: Distance dependent electron transmission through oligoprolines. Bioelectrochemistry 2010, 87, 21–27.

(19). Li W-Q; Huang B; Huang M-L; Peng L-L; Hong Z-W; Zheng J-F; Chen W-B; Li J-F; Zhou X-S Detecting Electron Transport of Amino Acids by Using Conductance Measurement. Sensors 2017,17, 811.

(20). Hihath J; Tao N Rapid measurement of single-molecule conductance. Nanotechnology 2008,19, 265204. [PubMed: 21828676]

(21). Xu BQ; Tao NJ Measurement of single-molecule resistance by repeated formation of molecular junctions. Science 2003, 301, 1221–1223. [PubMed: 12947193]

(22). Venkataraman L; Klare JE; Nuckolls C; Hybertsen MS; Steigerwald ML Dependence of single-molecule junction conductance on molecular conformation. Nature 2006, 442, 904–907. [PubMed: 16929295]

(23). Quek SY; Venkataraman L; Choi HJ; Louie SG; Hybertsen MS; Neaton JB Amine-gold linked single-molecule circuits: Experiment and theory. Nano Lett. 2007, 7, 3477–3482. [PubMed: 17900162]

(24). Venkataraman L; Klare JE; Tam IW; Nuckolls C; Hybertsen MS; Steigerwald ML Single-Molecule Circuits with Well-Defined Molecular Conductance. Nano Lett. 2006,6,458–462. [PubMed: 16522042]

(25). Chen F; Li XL; Hihath J; Huang ZF; Tao NJ Effect of anchoring groups on single-molecule conductance: Comparative study of thiol-, amine-, and carboxylic-acid-terminated molecules. J. Am. Chem. Soc 2006,128, 15874–15881. [PubMed: 17147400]

(26). Ahn S; Aradhya SV; Klausen RS; Capozzi B; Roy X; Steigerwald ML; Nuckolls C; Venkataraman L Electronic transport and mechanical stability of carboxyl linked single-molecule junctions. Phys. Chem. Chem. Phys 2012,14, 13841–13845. [PubMed: 22850823]

(27). Cordes M; Kottgen A; Jasper C; Jacques O; Boudebous H; Giese B Influence of amino acid side chains on long-distance electron transfer in peptides: electron hopping via “stepping stones”. Angew. Chem. Int. Ed 2008, 47, 3461–3.

(28). Guo C; Yu X; Refaely-Abramson S; Sepunaru L; Bendikov T; Pecht I; Kronik L; Vilan A; Sheves M; Cahen D Tuning electronic transport via hepta-alanine peptides junction by tryptophan doping. Proc. Natl. Acad. Sci. U.S.A. 2016,113, 10785–90. [PubMed: 27621456]

(29). Nagahara LA; Thundat T; Lindsay SM Preparation and Characterization of STM Tips for Electrochemical Studies. Rev. Sci. Instrum 1989, 60, 3128–3130.

(30). Kamenetska M; Koentopp M; Whalley A; Park YS; Steigerwald M; Nuckolls C; Hybertsen M; Venkataraman L Formation and Evolution of Single-Molecule Junctions. Phys. Rev. Lett 2009,102, 126803. [PubMed: 19392306]

(31). Boumrah D; Suckling CJ; Dufton MJ Characteristics of the peptidase activity contained in Taiwan cobra (Naja naja atra) venom. Toxicon 1993, 31, 1293–1303. [PubMed: 8303723]

(32). Zang Y; Pinkard A; Liu Z-F; Neaton JB; Steigerwald ML; Roy X; Venkataraman L Electronically Transparent AuN Bonds for Molecular Junctions. J. Am. Chem. Soc 2017,139, 14845–14848. [PubMed: 28981277]

(33). Park YS; Whalley AC; Kamenetska M; Steigerwald ML; Hybertsen MS; Nuckolls C; Venkataraman L Contact Chemistry and Single-Molecule Conductance: A Comparison of Phosphines, Methyl Sulfides, and Amines. J. Am. Chem. Soc 2007,129, 15768–15769. [PubMed: 18052282]

(34). Brandbyge M; Mozos JL; Ordejon P; Taylor J; Stokbro K Density-functional method for nonequilibrium electron transport. Phys. Rev. B 2002, 65, 165401.

(35). Neaton JB; Hybertsen MS; Louie SG Renormalization of molecular electronic levels at metal-molecule interfaces. Phys. Rev. Lett 2006, 97, 216405. [PubMed: 17155759]

(36). Perdew JP; Burke K; Ernzerhof M Generalized Gradient Approximation Made Simple. Phys. Rev. Lett 1996, 77, 3865–3868. [PubMed: 10062328]

(37). Soler JM; Artacho E; Gale JD; Garcia A; Junquera J; Ordejon P; Sanchez-Portal D The SIESTA method for ab initio order-N materials simulation. J. Phys. Condens. Matter 2002, 14, 2745–2779.

(38). Liu Z-F; Wei S; Yoon H; Adak O; Ponce I; Jiang Y; Jang W-D; Campos LM; Venkataraman L; Neaton JB Control of Single-Molecule Junction Conductance of Porphyrins via a Transition-Metal Center. Nano Lett. 2014,14, 5365–5370. [PubMed: 25111197]

(39). Wierzbinski E; Yin X; Werling K; Waldeck DH The Effect of Oxygen Heteroatoms on the Single Molecule Conductance of Saturated Chains. J. Phys. Chem. B 2013, 117, 4431–4441. [PubMed: 23101934]

(40). Eckshtain-Levi M; Capua E; Refaely-Abramson S; Sarkar S; Gavrilov Y; Mathew SP; Paltiel Y; Levy Y; Kronik L; Naaman R Cold denaturation induces inversion of dipole and spin transfer in chiral peptide monolayers. Nat. Commun 2016, 7, 10744. [PubMed: 26916536]

(41). Miller SE; Watkins AM; Kallenbach NR; Arora PS Effects of side chains in helix nucleation differ from helix propagation. Proc. Natl. Acad. Sci. U.S.A. 2014,111, 6636–6641. [PubMed: 24753597]

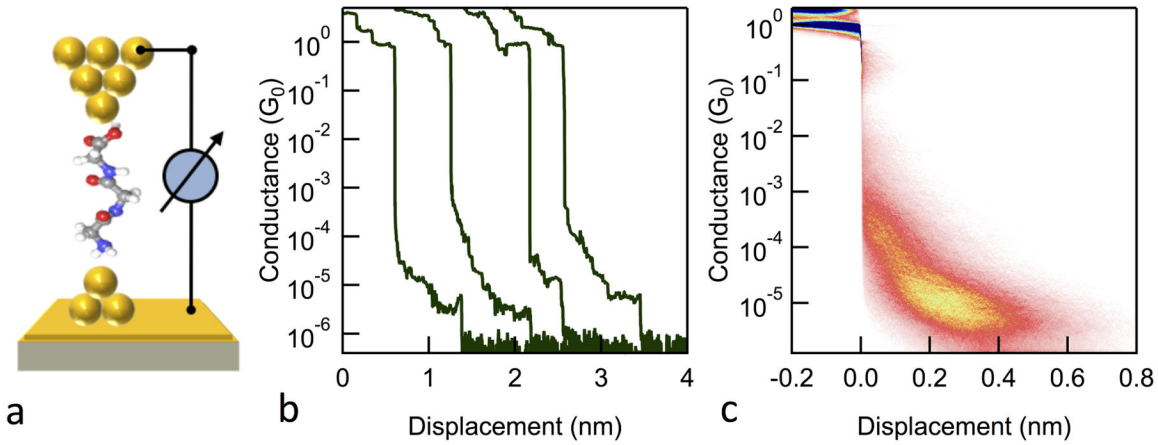

Figure 1:

(a) Schematic of a single peptide junction showing **AAA** bridging two gold electrodes. (b) Sample conductance versus displacement traces for **AAA** measured in water at pH 7 using an applied bias of 500 mV. (c) 2D conductance-displacement histogram constructed by overlaying all measured **AAA** conductance traces after aligning the displacement at 0.5 G_0 and using logarithmic bins (100 per decade) along the conductance axis and linear bins (100/Å) along the displacement axis. The molecular junction extends by about 0.5 nm beyond the rupture.

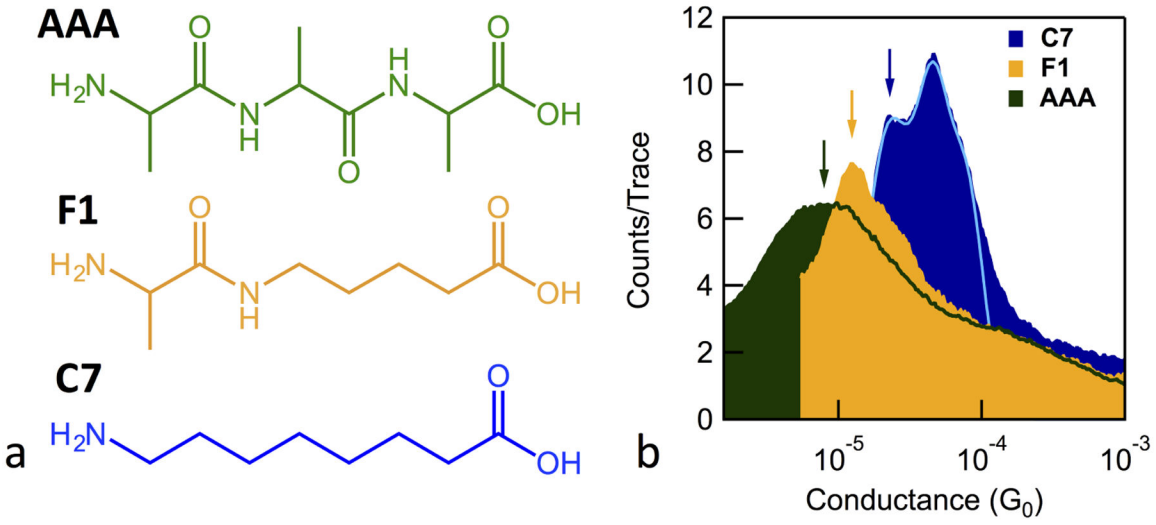

Figure 2:

(a) Structure of **AAA, F1** and **C7**. (b) 1D conductance histograms created from all measurement traces of **AAA, F1** and **C7** showing that conductance decreases as the number of peptide bonds in the backbone increases. Light blue trace shows a fit to the 1D histogram peak for **C7** the sum of three Gaussians. The arrows point to the single-molecule junction conductance. 1D conductance histograms are constructed using logarithmic bins (100 per decade) without any data selection.

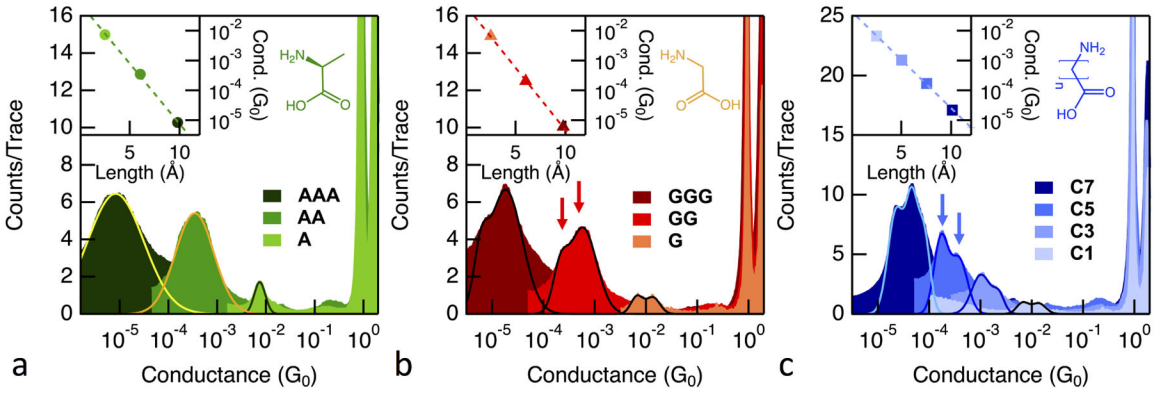

Figure 3:

Conductance histograms for (a) oligoalanine (b) oligoglycine and (c) alkanes. All histograms are generated from all measured traces without data selection. Solid lines indicate Gaussian (or multi-Gaussian) fits to the data. Arrows in (b) and (c) point to the single and double molecular junction peaks for **GG** and **C5** respectively. Note that **G** and **C1** are the same molecule. In set: (right) Structure of alkane/peptides. (left) Measured single-molecule conductance (histogram peak) versus calculated molecular junction length shown on a semi-logarithm scale along with a linear fit to the data.

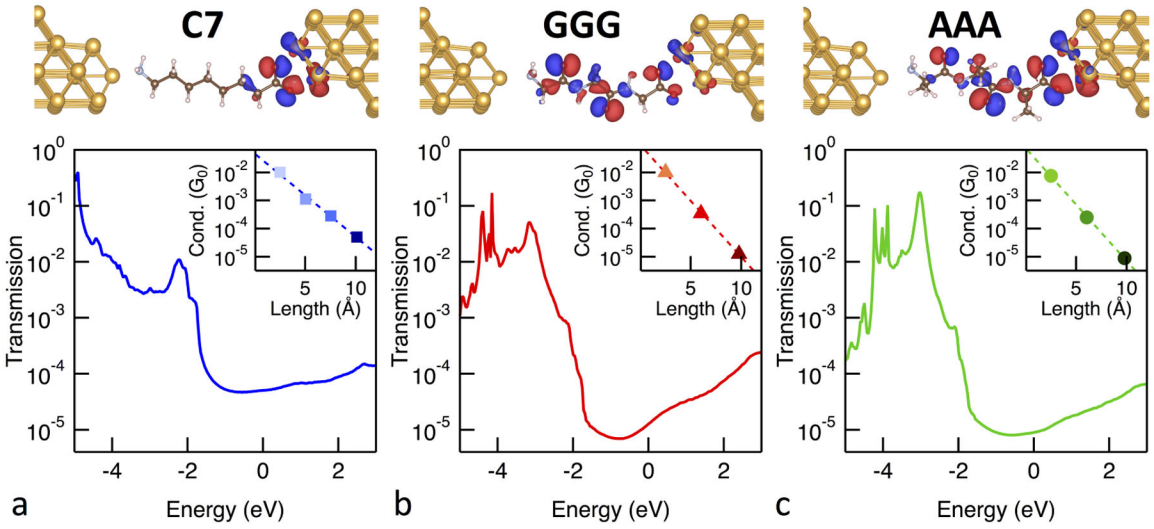

Figure 4:

Zero-bias transmission functions, computed with a generalized DFT+Σ method for the case of covalent binding, as described in the text, for (a) **C7**, (b) **GGG** and (c) **AAA**, as a function of energy (eV) relative to the Fermi energy, E_F. Inset: Calculated conductance versus calculated molecular junction length. For each system, the eigenchannels associated with the highest occupied peak at −2 eV are shown as well. While for **C7** the main charge distribution is along the covalent Au-COO^- binding, for both **GGG** and **AAA** further wavefunctions localization on the peptide-bonds along the peptide backbone is shown.